ChemComm

Accepted Manuscript

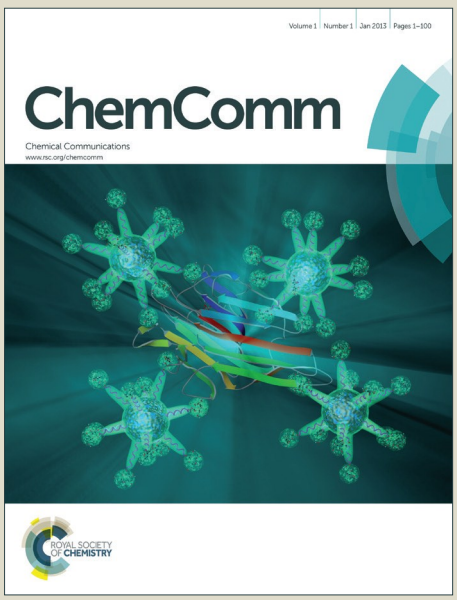

ROYAL SOCIETY OF CHEMISTRY

www.rsc.org/chemcomm

ChemComm

COMMUNICATION

Single-Material Solvent-Sensitive Actuator from Poly(ionic liquid) Inverse Opals based on Gradient Dewetting

Received 00th January 20xx,
Accepted 00th January 20xx

DOI: 10.1039/x0xx00000x

www.rsc.org/

Hua Wu[a,b]†, Minxuan Kuang[b]†, Liying Cui[a]†, Di Tian[b], Minghui Wang[a], Guoyou Luan[*,a], Jingxia Wang[*,b] and Lei Jiang[b]

A novel and reversible single-material solvent-sensitive actuator was developed from poly(ionic liquid) inverse opals based on gradient wetting/dewetting process combining with the strong hydrogen bonding interaction between solvent and the polymer. This work will provide an important insight for the design and fabrication of novel-type solvent-actuator materials.

In nature, many organisms take response to the environment water or solvent for actuation[1c]. Typically, the seed dispersal units of pinecones, wheat awns and seedpods remain closed state when on the tree or under wet environment, and they are able to open and release the seeds as dry out. Inspired by these smart organisms, various stimulus actuators[1-10] are fabricated from the passive -active bilayer structure, with responsive materials as the active layer, combining with the passive material as substrate. These smart materials are able to generate mechanical work under external stimuli, such as light[3b,4-5], electricity[2c-d], moisture[1a,1d,9], solvent[2a,3a,9], magnetism[8] and heat[6], having the potential applications in microrobotic,[8b] artificial muscles[2c,8], energy generators[1a,1d] and etc. Recently, one kind of simple actuator derived from gradient[1d] or single materials[1a] exerts great research interest based on the inhomogeneous swelling/shrinking within the films owing to efficiently overcoming the stress restriction of bilayer-actuator. It is of especial importance for the development of simple, economy sensing material/devices. In this paper, we demonstrated a single-material solvent-sensitive actuator based on the gradient wetting/dewetting process. The sample is fabricated from single-material of poly(ionic liquid) (PIL) inverse opals, one kind of excellent candidate for actuator materials since it possesses the bulk organic counter anions and can interact with a variety of organic solvents[3a]. Furthermore, the porous structure of inverse opals[11] gives rise to a fast responsiveness by accelerating the internal mass transport and the large-scale actuation arising from high compressibility. The as-prepared PIL actuator demonstrates bending angle of 140^0 in 4 s. The actuator magnitude/rate of the PIL inverse opals can be modulated by solvent kinds and the PIL composition, as can be attributed to the gradient wetting/dewetting behavior of the solvents on the PILs combined with strong hydrogen bonding interaction between PIL and solvents. This fabrication of single-material bending actuator will impose an important insight for the design and manufacture of novel and advanced solvent-actuator.

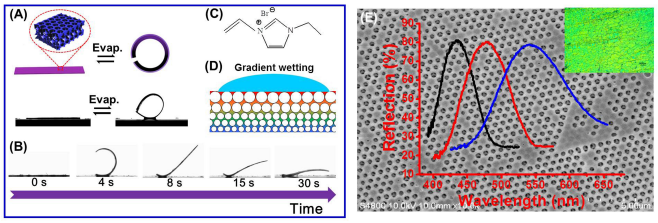

Figure 1. (A) Scheme for the actuating behavior of solvent-sensitive PIL inverse opals based on wetting/dewetting process, the fully wetting sample can be actuated upon gradient dewetting arousing from solvent evaporation. (B) *In-situ* photos for a typical actuating process of the fully wetting sample based on gradient dewetting. (C) Chemical structure of the used IL monomer: 1-vinyl-3-ethylimidazolium bromide. (D) SEM image of the sample, the inserts are the optic photo (upper right) and the UV-vis reflection spectra of the sample.

Figure 1A,B(and Figure S1) shows a typical reversible actuating process of the as-prepared PIL inverse opals accompanied with a gradient solvent evaporation. At first, the inverse opals are straight and flat when being fully swollen in the solvent. Subsequently, only one side of the sample deforms and tilts upward together with gradient dewetting aroused from the solvent evaporation. The curvature of sample grows rapidly and causes the film rolling into a circle with further solvent evaporation. Afterwards, the curvature of sample gradually falls and the film reverts to the original flat state with solvent complete evaporation. In the whole actuator process, the gradient wetting/de-wetting property (inserted) of the solvent on the PIL ensures an inhomogeneous

a.College of Resources and Environment, Jilin Agricultural University, Changchun 130118, P. R. China, corresponding E-mail: 957478465@qq.com.
b.Laboratory of Bio-Inspired Smart Interface Sciences, Technical Institute of Physics and Chemistry, Chinese Academy of Sciences, Beijing 100190, P. R China
Corresponding E-mail: jingxiawang@mail.ipc.ac.cn,wangzhang@iccas.ac.cn
† H. Wu, M. X. Kuang and L. Y. Cui contribute equal to this article.
Electronic Supplementary Information (ESI) available: [details of any supplementary information available should be included here]. See DOI: 10.1039/x0xx00000x

swollen/shrinkage of the polymer segment in the solvent, forming a primary driven force and affecting the actuator magnitude/rate, the reversibility, and the resulted application performance. The free-standing actuator of PIL inverse opals was manufactured by infiltration of the polymerizable ionic liquid monomer of 1-vinyl-3-ethylimidazolium bromide into the interstice of poly(St-MMA-AA) PC template, subsequent photo-polymerization and the template removal. The fabrication method is similar to the general fabrication process of opal[11a] and inverse opal[11b] in literature method. Figure 1D shows SEM image of the as-prepared PIL inverse opals, a clearly periodic porous structure and iridescent structure color (inserted) indicate a successful fabrication of PIL inverse opals. The stopband position of the inverse opals shifts from 440, to 480, to 530 nm with the increased particle diameter from 210, to 250, to 330 nm in the PC templates. The FTIR spectra of sample showed unique characteristic peak of 1657, 1550, 1450, and 1164 cm^{-1} in Figure S2A corresponding to the vibration of imidazole ring, confirming the formation of PIL inverse opals.

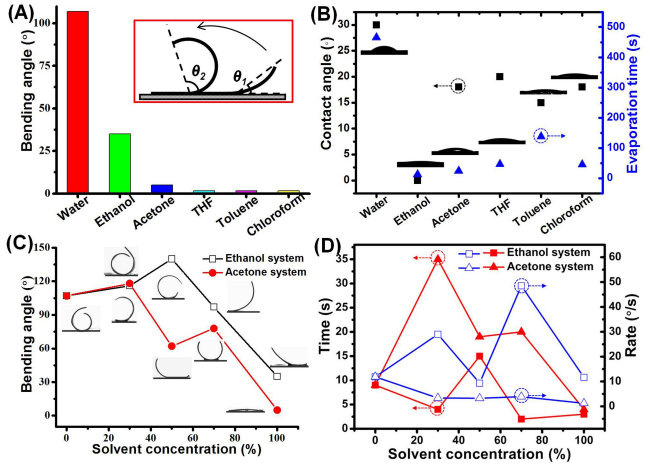

Figure 2. (A,C) Bending angle of the sample at different solvent system, the bending angle of sample during the actuator process is calculated as inserted scheme. (B) The contact angle and the evaporation time of various solvents on the sample. (D)Time taken for the sample approaching the largest bending angle in different solvent system. In this case, the sample is made from 100% PIL inverse opals.

Figure 2 presents the bending angle of the as-prepared PIL inverse opals (containing of 100% PIL) upon various solvent conditions. The bending angle is defined from the intersected angle between the linkage line and the basic line (inserted in Figure 2A). Linkage line is formed based on the tilted end of the sample and the support point. Clearly, the actuators exhibit distinct bending behaviors when being taken out from various solvents. Little bending behavior occurs to the sample when being out from THF, toluene and chloroform in Figure 2A. In contrast, an obviously bending behavior can be observed for sample from water, ethanol, and acetone with bending angle of 107°, 35°, 5° respectively. To understand what affecting the distinct actuator behavior toward different solvents, we investigate an *in-situ* wetting/dewetting process of various solvents upon the PIL film as shown in Figure 2B and S2. In this case, the wetting/dewetting property is characterized by contact angle (CA) of solvent on the sample and the evaporation rate respectively[13]. It is found that CA falls from 32°, to 18°, to 0° for water, acetone and ethanol on the samples respectively (Figure 2B), indicating an increased wetting process and an enhanced interaction force between solvent and polymer. Otherwise, the evaporation time decreases from 465, to 24, to 12 s for the solvent changing from H_2O, to acetone, and to ethanol respectively, implying an increased dewetting property for the solvent upon the sample. Obviously, the increased wetting/dewetting phenomenon is corresponding to the decreased bending angle of the sample out from various solvents (in Figure 2A). It can be attributed that the rapid wetting/dewetting process (of solvent) prefers to a complete swell/deswell mode, rather than an inhomogeneous swell/shrink of the sample and the corresponding actuator behavior.The latter one is a basic driven force for the actuator property. Notably, little bending angle is observed for THF, toluene and chloroform in Figure 2A, this can be attributed to non-dissoluble/non-swell for the solvent to the polymer[1d], implying no tensile force in the process (see supporting data). In contrast, better swell but non-dissoluble property is observed for the polymer in acetone, ethanol, and water system. In this case, actuating property of single-material actuator mainly depends on the gradient wetting/dewetting, that induces an inhomogeneous swell/deswell and triggers the actuator action of the corresponding polymer.

Interestingly, the actuator behavior of PILs can be modified using mixing solvent of water and acetone/ethanol as shown in Figure 2C, Figure S5-S9. It was found that bending angle of the actuator varies from 107°, to 106°, to 140°, to 97°, and to 35° with the increased ethanol ratio in water from 0%, to 30%, to 50%, to 70%, and to 100%, respectively. Similarly, the bending angle changes from 107°, to 118°, to 62°, to 78°, and to 5° when raising the acetone ratio in water from 0%, to 30%, to 50%, to 70%, and to 100% respectively. The largest bending angle is observed at 140° in the ethanol-water (1:1) system, and the smallest bending angle is 5° in the pure acetone system. The reinforced actuator amplitude aroused from the mixing solvent mainly can be attributed to an enhanced hydrogen bonding interaction between PIL and various solvents. Meantime, the improved evaporate solvent flux originated from acetone/ethanol also provides an additional driven force for the bending process of the sample, which relieves the effect from gravity force and the resistance force during the bending process. Additionally, the mixing solvent changes the condition of gradient wetting (see Figure S3 and S4). For instance, the addition of water into acetone/ethanol greatly slows the evaporate rate, resulting in the transition from complete wetting to gradient wetting. All of these contributes to the modulation of actuator behavior of the samples.

Similarly, the mixing solvent system affects the actuator rate of the samples as shown in **Figure 2D** and Figure S10-S11. Where, the actuator rate is characterized by the time taken at the largest bending angle, or the bending angle in 1 second. It is found that a shorter actuator time taken in ethanol system

than that in acetone on. The actuator time changes from 9, to 35, to 19, to 20, and to 4 s, respectively. And the actuation rate shifts from 11.89, to 3.37, to 3.26, to 3.9, and to 1.25 °/s for the mixing solvent with growing ratio of acetone in water from 0, to 30%, to 50%, to 70%, and to 100%. In comparison, the actuator time modulates from 9, to 4, to 15, to 2, and to 3 s, and the actuation rate jumps from 11.89, to 29, to 9.33, to 48.5, and to 11.67 °/s with increased ethanol ratio in water from 0, to 70%, to 50%, to 70%, and to 100%. It is found that the fastest response rate occurs for the sample at the 30% ethanol system. Notably, the samples took 2 s to reach the bending angle of 97° in the 30% ethanol-water mixture, respectively. The increased actuator rate can be attributed to the enhanced hydrogen bond interaction and the improved evaporation rate owing to the introduction of acetone/ethanol. Notably, the pure acetone/ethanol system shortens the response time, but it yields small bending angle arousing from the short gradient wetting time. Accordingly, the suitable selection of solvent system is very important for the resultant application performance of actuator materials.

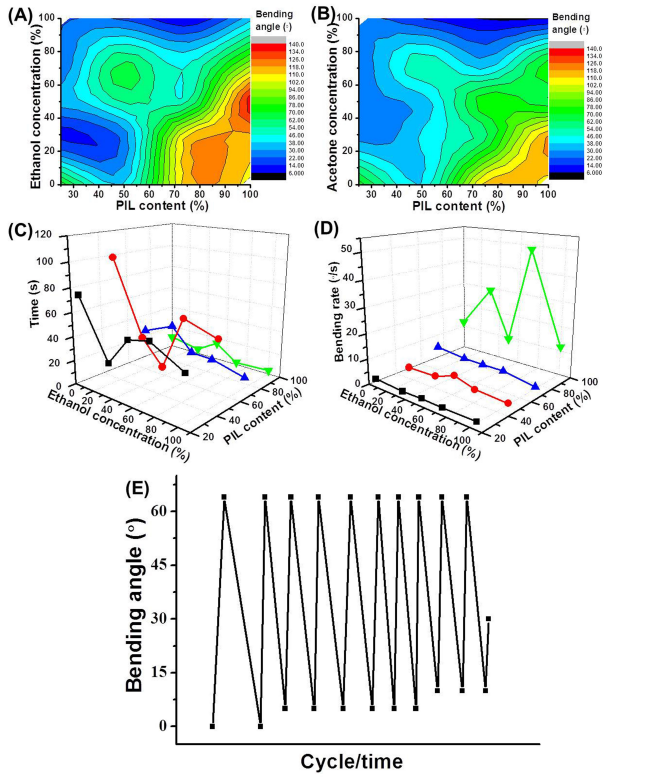

Figure 3. The largest bending angle for various PIL inverse opals in (A) ethanol and (B) acetone system. (C) Response time for the samples achieving the largest bending angle and (D) response rate of the sample containing 100% PIL at different ethanol system. (E) Reversible transition property of the PIL actuator (containing of 75% PIL) upon the gradient wetting/dewetting process.

Not only the solvent kinds, the polymer composition of the PIL inverse opals also affects the bending angle of the actuators as shown in **Figure** 3A-D. Generally, the inverse opals (with 100% PIL) have relative larger bending angle in the ethanol/acetone system (Figure 3A,B). Decreased PIL content results in an obvious fall of bending angle of the samples. The values change from 140°, to 49°, to 56°, and to 34° for the sample with a decreased PIL content from 100%, to 75%, to 50%, and to 25% in the 50% ethanol solvent system, respectively. Furthermore, the composition of the actuator polymer also influences the bending rate of the sample. The actuation time for the largest bending angle of the sample moves from 15, to 17, to 15, and to 48 s, and the actuation rate shifts from 9.33°/s, to 2.88°/s, to 3.73°/s, and to 0.71°/s for the sample with PIL content dropping from 100%, to 75%, to 50%, and to 25% in 50% ethanol solvent system respectively. Clearly, both the shortest time and the fastest bending rate occur to the sample prepared from 100% PIL whether various solvent system. A great decrease of the bending rate is observed when increased the PMMA content in PIL inverse opals. These indicate that the decreased PIL in the polymer segment degrades the bending rate owing to the weaken hydrogen bonding interaction between the actuator polymer and solvent. In our case, Br^- anions and H protons in polymer chains of PIL form hydrogen bonding with H protons and O atoms in solvent molecule. The intermolecular hydrogen bonding provides a tractive force during the solvent evaporation process.[1a] On the other hand, a deformation force is generated in the actuators due to the elastic bending deformation. This force gradually grows with the increased bending deformation. The actuators produced the largest bending angle when the tractive force and deformation force reach balance[3a]. But the curvature of the films gradually drops with the decreased PIL in the samples. These varied actuating behaviors imply that the solvent system and the composition of the actuator polymer will exert important effects on the performance of actuators. **Figure 3E** shows that the actuators can retain reversibility for more than 10 cycles. The largest bending angle drops by half at eleventh cycle.

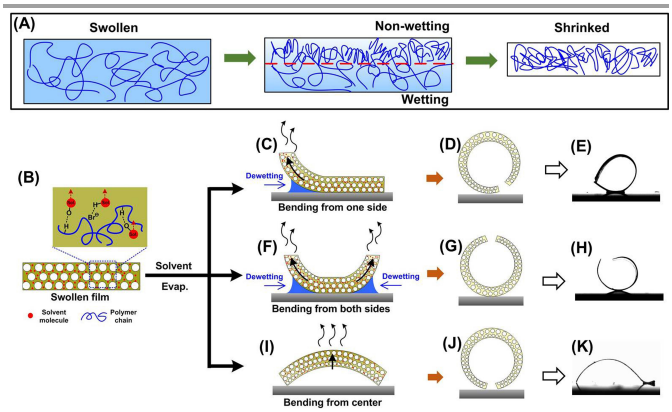

Figure 4. Schematic for the typical actuator process of single-material PIL inverse opals. (A) Three existing states of the polymer segments(from left to right): full swollen, gradient dewetting (gradient swollen), complete shrinkage state. Where, the gradient dewetting is a crucial state for the single-material actuator. (B) Detailed scheme for the full swollen state. Where, the strong hydrogen bonding exists between the solvent and polymer segment. (C, F and I) Three kinds of dewetting state of the sample, (D, G, J) the corresponding deformation way and (E, H, K) the final bending behavior of sample.

In fact, in a typical single-material actuator system, the solvent actuating behavior such as bending amplitude/rates of the actuators mainly depends on an inhomogeneous swell/shrink[1a,1c] for the polymer segment in the solvent, which is induced from the gradient wetting/dewetting process of

solvent toward the samples as shown in **Figure 4A** (middle). The wetting part of polymer segment makes it full extending toward an elastic network structure, forming the hydrogen bonding interaction among the polymer and solvent. While the non-wetting part keeps an entanglement frozen state[12]. The inhomogeneous swell/deswell of the bulk polymer segment induces a tensile production between the top dewetting part and the bottom wetting part, forming an upward/downward bending of the sample. Similarly, the dewetting (non-wetting) part causes a shrinkable polymer segment, non-dewetting (wetting) part keeps the swollen ones. The inhomegeneous swell/shrink overcomes the gravity force and drives the films lifting up. In contrast, the fast wetting/dewetting process restricts the formation of inhomogeneous shrink/swell, leading to a failed actuator behavior. Figure 4B-K presents a possible explanation for the different bending behavior of PIL inverse opals during the solvent evaporation process. At first, the films are fully swollen by the solvent, the strong hydrogen bonding integrates between the polymer and solvent molecules in Figure 4B. With the solvent evaporation, the frontier of the liquid retracts from the side/top part to the middle/bottom one of the film, causing a shrinkable state started from the upper/side to the bottom/center part, inducing an upward bending of the sample. With further solvent evaporation, the tractive force induced by the convective flow moves along the frontier of the liquid. The film enhances its bending angle and finally rolls into a circle. During the bending process, the tractive force is larger than the sum of gravity and deformational force all the time. Therefore, the film could retain its bending state. Finally, the inhomogenous dewetting turns to a homogeneous dry, and the tensile force decreases/disappears, leading to a gradual return toward the original flat state. Notably, a strong capillary force exists between film and substrate resulted from the solvent among them, which pins the sample toward the substrate[12c]. But it also slows the solvent evaporation in the lower part of the sample, plays an important role on the formation of gradient dewetting in Scheme 4A(middle).

In the experiments, three bending situations occur to the actuator films as shown in Figure 4B-K: the bending behavior starts from the film ends (Figure 4C,F) and the middle parts (Figure 4I). The different bending situations could be attributed to the varied dewetting cases and the convective flow interaction, determining the position of tractive force. The tractive force is firstly generated at the film ends owing to the fast evaporation flow there, resulting in a corresponding dewetting, fast shrink and an upward bending from one/two end of the film. The subsequent evaporated solvent induces the further shrinkable of the sample, contributing to the enhanced bending behavior and circle formation in the Figure 4D and G. Additionally, bending from the middle part and the arc-like deformation In Figure 4J can be understood that an inhomogeneous swell/dewetting occur toward the middle part of the sample although that the rapid evaporation started from the two end fails to induce the inhomogeneous shrink.

In conclusion, a reversible single-material solvent-response actuator can be achieved from the PIL inverse opals based on the gradient wetting/dewetting process. The sample demonstrates 140° bending in 4 s. Which will provide an important insight for the design and fabrication of novel actuator materials.

J. X. Wang would like to thank the NSFC (Grant no. 51373183, 51503214, 91127029, 21074139 and 50973117) for the financial support. M. H Wang thanks the support from the Doctor funding (No. 20218).

Notes and references

[1] (a) M. M. Ma, L. Guo, D. G. Anderson, R. Langer, *Science* 2013, **339**, 186; (b) Z. Q. Pei, Y. Yang, Q. M. Chen, E. M. Terentjev, Y. Wei and Y. Ji, *Nat. Mater*. 2014, **13**, 36; (c) L. Ionov, *Adv. Funct. Mater*. 2013, **23**, 4555; (d) Q. Zhang, J. W. C. Dunlop, X. L. Qiu, F. H. Huang, Z. B. Zhang, J. Heyda, J. Dzubiella, M. Antonietti, J. Y. Yuan, *Nat. Commun*. 2014, **5**, 4293.

[2] (a) A. Sidorenko, T. Krupenkin, A. Taylor, P. Fratzl, J. Aizenberg, *Science* 2007, **315**, 487; (b) P. Fratzl, F. G. Barth, *Nature* 2009, **462**, 442; (c) R. Shankar,T. K. Ghosh and R. J. Spontak, *Adv. Mater*. 2007, **19**, 2218; (d) P. N. Chen, S. S. He, Y. F. Xu, X. M. Sun, H. S. Peng, *Adv. Mater.* 2015, **27**, 4982.

[3] (a) Q. Zhao , J. Heyda , J. Dzubiella , K. Täuber , J. W. C. Dunlop and J. Y. Yuan, *Adv. Mater*. 2015, **27**, 2913; (b) L. D. Zhang and Panc˘e Naumov, *Angew. Chem. Int. Ed*. 2015, **54**, 8642; (c) F. Zhou, W. Shu, M. E. Welland, W. T. S. Huck, *J. Am. Chem. Soc*. 2006, **128**, 5326; (d) M. R. Islam, X. Li, K. Smyth, M. J. Serpe, *Angew. Chem. Int. Ed.* 2013, **52**, 10330.

[4] (a) W. Wu, L. M. Yao, T. S.Yang, R. Y. Yin, F. Y. Li and Y. L.Yu, *J. Am. Chem. Soc*. 2011, **133**, 15810; (b) M. Y. Ji, N. Jiang, J. Chang and J. Q. Sun, *Adv. Funct. Mater*. 2014, **24**, 5412; (c) T. Takeshima, W. Y. Liao, Y. Nagashima, K. Beppu, M. Hara, S. Nagano and T. Seki, *Macromolecules* 2015, **48**, 6378.

[5] (a) L. Wang and Q. Li, *Adv. Funct. Mater.* 2016, **26**, 10; (b) L. Wang, K. G. Gutierrez-Cuevas, H. K. Bisoyi, J. Xiang, G. Singh, R. S. Zola, S. Kumar, O. D. Lavrentovich, A. Urbas and Q. Li, *Chem. Commun.* 2015, **51**, 15039; (c) R. Sun, C. M. Xue, X. Ma, M. Gao, H. Tian and Q. Li, *J. Am. Chem. Soc.* 2013, **135**, 5990; (d) J. Ma, Y. N. Li, T. White, A. Urbas and Q. Li, *Chem. Commun.* 2010, **46**,3463.

[5] (a) E. Lee, D. Kim, H. Kim and J. Yoon, *Sci. Rep.* 2015, **5**, 10124; (b) W. E. Lee, Y. J. Jin, L. S. Park and G. Kwak, *Adv. Mater.* 2012, **24**, 5604; (c) K. M. Lee, H. Koerner, R. A. Vaia, T. J. Bunninga and T. J. White, *Soft Matter* 2011, **7**, 4318.

[6] (a) C. Yao, Z. Liu, C. Yang, W. Wang, X. J. Ju, R. Xie and L. Y. Chu, *Adv. Funct. Mater.* 2015, **25**, 2980; (b) V. Stroganov, M. Al-Hussein, J. U. Sommer, A. Janke, S. Zakharchenko and L. Ionov, *Nano Lett*. 2015, **15**, 1786; (c) S. H. Jiang, F. Y. Liu, A. Lerch, L. Ionov and S. Agarwal. *Adv. Mater*. 2015, **27**, 4865; (d) K. Miyamae, M. Nakahata, Y. Takashima, A. Harada, *Angew. Chem. Int. Ed.* 2015, **54**, 8984.

[7] (a) M. J. Liu, X. L. Liu, J. X. Wang, Z. X. Wei and L. Jiang, *Nano Res.* 2010, **3,** 670; (b) G. A. Sotiriou, C. O. Blattmann and S. E. Pratsinis, *Adv. Funct. Mater.* 2013, **23**, 34.

[8] (a) K. Zhang, A. Geissler, M. Standhardt, S. Mehlhase, M. Gallei, L. Q. Chen and C. M. Thiele, *Sci. Rep*. 2015, **5**, 11011; (b) B. Li, T. Du, B. U, J. Van der Gucht, F. Zhou. *Small* 2015, **11**, 3494; (c) B. Li, T. Du, B. Yu, J. van der Gucht and F. Zhou, *Small* 2015, **28**, 3494.

[9] Y. Q. Gu and N. S. Zacharia, *Adv. Funct. Mater*. 2015, **25**, 3785.

[10] (a) J. X. Wang, Y. Q. Wen, H. L. Ge, Z. W. Sun, Y. M. Zheng, Y. L. Song, L. Jiang, *Macromol. Chem. Phys.* 2006, **207**, 596-604; (b) J. M. Zhou, H. L. Li, L. Ye, J. X. Wang, T. Zhao, L. Jiang, Y. L. Song, *J. Phys. Chem. C.*, 2010, **114**, 22303; (c) J. X. Wang, Y. Z. Zhang, S. T. Wang, Y. L. Song, L. Jiang, *Acc. Chem. Res*. 2011, **44**, 405; (d) T. Ding, F. Wang, K. Song, G. Q. Yang, C. H. Tung, *J. Am. Chem. Soc.* 2010, *132*, 17340; (e) M. S. Wang, L. He, Y. D. Yin, *Mater. Today* 2013, **16**, 110; (f) Q. Zhang, M. Janner, L. He, M. S. Wang, Y. X. Hu, Y. Lu, Y. D. Yin, *Nano Lett.* 2013, **13**, 1770.

[11] (a) J. S. Leng, X. Lan, Y. J. Liu, S. Y. Du, *Prog. Mater. Sci*. 2011, 1077; (b) Y. Osada, H. Okuzaki, H. Hori, *Nature* 1992, **355**, 242; (c) F. Greco, V. Domenici, A. Desii, E. Sinibaldi, B. Zupancic, B. Zalar, B. Mazzolai, V. Mattoli, *Soft Matter* 2013, **9**, 11405.

[12] (a) Y. Tian, B. Su, L. Jiang, *Adv. Mater.* 2014, 26, 6872; (b) Y. Tian, L. Jiang. *Nat. Mater.* 2013, **12**, 291; (c) S. T. Wang, K. S. Liu, X. Yao, L. Jiang, *Chem. Rev.* 2015, **115**, 8230..

